ChemistrySelect

Research Article
doi.org/10.1002/slct.202201223

Chemistry Europe
European Chemical Societies Publishing

www.chemistryselect.org

Energy Technology & Environmental Science

Synthesis of Novel Artemisinin Derivatives and Their Electrochemical Properties

Meryem Esen,[a] Emrah Kavak,[a] Omruye Ozok-Arici,[b] Berdan Ulas,[c] Hilal Kivrak,*[b, d] and Arif Kivrak*[e]

In present, new artemisinin-based organic compounds (**1**–**6**) are designed and synthesized in excellent yields (up to 97%) via Steglich Esterification reactions. All new artemisinin derivatives are tested as anode catalysts for hydrazine electrooxidation reactions with electrochemical methods in 1 M KOH/0.5 M N_2H_4 solution. Hybrid **molecule 1** exhibits the best catalytic activity in hydrazine electrooxidation reaction with 2.28 mA cm^{-2} value. Moreover, response surface methodology (RSM) is applied to investigate of optimum electrode conditions. By using optimum conditions, hydrazine electrooxidation is obtained as 3.55324 mA cm^{-2}. As a result, artemisinin-based hybrid compounds may be alternative, and next-generation anode catalyst for direct hydrazine fuel cells.

Introduction

Nowadays, renewable energy sources are the most important challenge all over the world due to the environmental impact associated with conventional sources and the energy crisis.[1] Fossil fuels are expensive and cause climatic effects like greenhouse gases. Nowadays, nuclear energy will be alternative for producing clean energy, but there are many question marks about the safety of nuclear facilities. The primary energy source is liquid fuels, petroleum and its by-products after the industrial revolution in the early nineteenth century. Although, natural gas has become main source of the producing of electricity and heat for industrial and domestic uses, 35.6% for petroleum, 28.6% for coal and 23.8% for natural gas were to be primary energy consumed worldwide at the end of 2007. The global perspective improved that sources of primary energy will not enough for next generations.[2]

Renewable energies and energy technologies have been gained very important for generation of clean energy.[3] New technologies are eco-friendly, needing renewable energy sources like sun, wind, water etc., and slightly cheaper than fossil sources.[4] Recently, a variety of batteries,[5] organic solar cells,[6] and fuel cells[7–9] have been investigated. Fuel cells may be the best way to formation of electrical energy by using chemical energy in cells. Fuel cells have a variety of potential applications such as using in power plants for industrial applications, vehicles and small devices.[10] Fuel cells have high efficiency of the chemical energy in the fuel to electrical energy, and they help to preserve the climate change due to lower carbon dioxide emissions. Moreover, they produce the only water as side product; they help to decrease the air pollutants.[11,12]

Hydrazine,[13] glucose,[14] formic acid,[15] ethanol,[8,16] and methanol[17–19] are the main fuel sources to producing electrical energy in fuel cells. Hydrazine, N_2H_4, is widely used in industry, explosives, rocket propellants, metal film manufactures, fuel cells, and photographic chemicals.[20] Hydrazine has superior properties such as; low cost, high energy density, higher performance and easy storage.[21]

Various catalysts have been developed for direct hydrazine fuel cells as an anode catalyst. For example, Cu–Ni,[22] PtCu/C,[23] NPGL,[24,25] AuPdDANCs,[26,27] Pd/CNT[28] were applied in fuel cells. In addition, Abdolmaleki *et al.* was used a simple direct hydrazine-hydrogen peroxide fuel cell based on the Au/C catalyzed for cathode and the Co@Au/C core-shell for anode.[29] Ojha *et al.* also reported that Fe_2MoC catalyst exhibits high catalytic activity with high stability (at least 2000 cycles).[30] As seen Table 1, the maximum peak values of metal-based catalysts for the hydrazine electrooxidation reaction are summarized in the literature.

Recent studies improved that organic materials were used as metal-free anode catalysts to electrooxidation in fuel cells. Er

[a] *M. Esen, E. Kavak*
Department of Chemistry, Faculty of Sciences,
Van Yuzuncu Yil University,
Van, 65080, Turkey
[b] *Dr. O. Ozok-Arici, Prof. H. Kivrak*
Eskisehir Osmangazi University,
Faculty of Engineering and Architectural Sciences,
Department of Chemical Engineering,
Eskisehir 26040, Turkey
[c] *Dr. B. Ulas*
Department of Chemical Engineering,
Faculty of Engineering, Van Yuzuncu Yil University,
Van, 65000, Turkey
[d] *Prof. H. Kivrak*
Translational Medicine Research and Clinical Center,
Eskisehir Osmangazi University,
26040 Eskisehir, Turkey
E-mail: hilalkivrak@gmail.com
[e] *Prof. A. Kivrak*
Eskişehir Osmangazi University,
Faculty of Sciences and Arts, Department of Chemistry,
Eskisehir 26040, Turkey
E-mail: arifkivrak@yahoo.com

Supporting information for this article is available on the WWW under https://doi.org/10.1002/slct.202201223

Table 1. Some examples for hydrazine electrooxidation in the literature.

Catalyst	Preparation	Maximum Peak (mA*cm^{-2})	Reference
poly(*P*-phenylenediamine/ZnO) (PpPD/ZnO)	dope	0.172	[32]
AuPd DANCs	co-reduction	9.57	[27]
VGNH-45	PECVD hydrothermal method	13	[33]
Benzothiophene	organic synthesis	4.95	[31]
MnO/N-C	dope	6.3	[34]
NiFe2O4-rGO	hydrothermal method	18.9	[35]
Flower-shaped CuO	dope	5.23	[36]

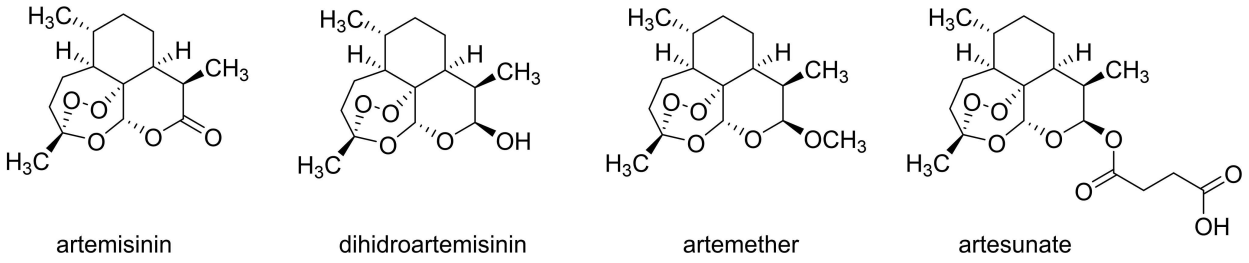

Figure 1. Artemisinin and known semi-synthetic derivatives

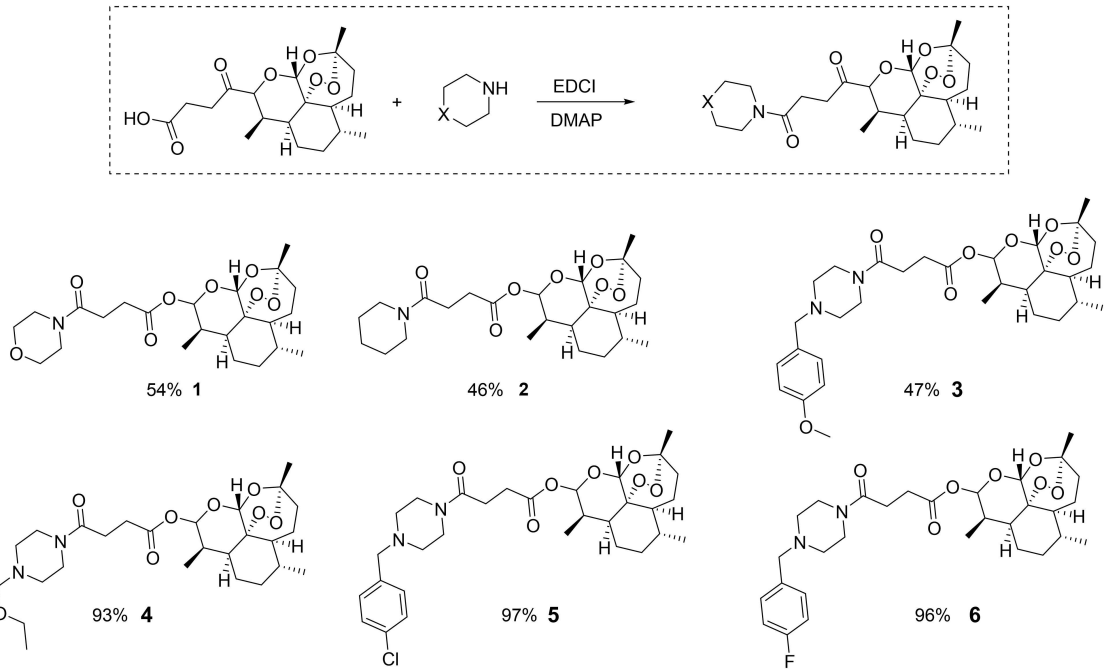

Figure 2. Synthesis of artemisinin-piperazine, artemisinin-piperidine and artemisinin-morpholine derivatives.

at al. were investigated that benzothiophene based organic catalyst exhibited the highest performance for hydrazine electrooxidation with 3.22 mA cm^{-2} value with the lowest charge transfer resistance.[31]

Heterocyclic molecules have played very critical roles for the design for new materials not only material science, but also biological applications. Carbazoles, thiophenes, indoles and pyridines are well known examples.[37–40] Moreover, heterocyclic compounds are core motifs for renewable energy sources due to their low molecular weight, flexibility, wide absorption bands, stable electrochemical stability, environmentally friendly, and reusability.[41,42]

Artemisinin a natural endoperoxide isolated from the plant *Artemisia annua L*, is widely used as an anti-malaria drug and their derivatives have anti-bacterial, anti-inflammatory, and anti-tumor activities.[27–30] Artemisinin exhibited greater activities than other antivirals, so it is known as the most effective drug in the treatment of malaria.[43,44] Semisynthetic derivatives

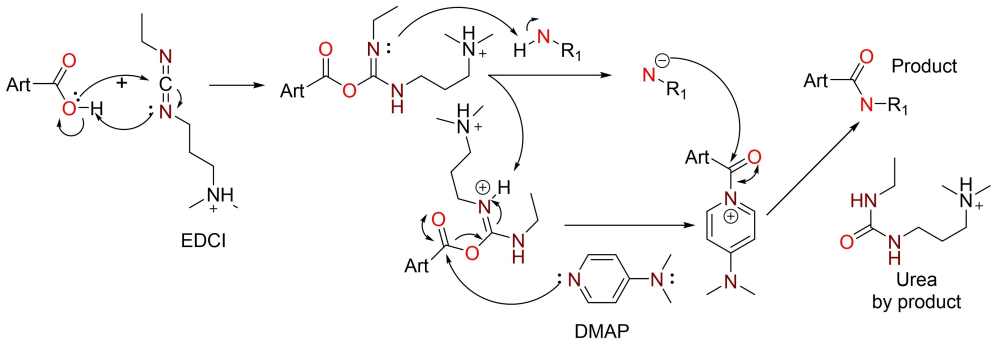

Figure 3. Possible reaction mechanism for the artemisinin hybrid molecules.

Table 2. Hydrazine electrooxidation properties of artemisinin-based catalysts.

Catalyst	Total Current of KOH (mA cm^{-2})	Total Current of Hydrazine (mA cm^{-2})	Normal Current, (mA cm^{-2})	Onset Potential (V)
DHA	0.10	0.98	0.88	−0.55
ART	1.43	1.45	0.02	−0.56
ARTS	0.10	1.64	1.54	−0.53
1	0.07	2.35	2.28	−0.51
2	0.21	1.11	0.90	−0.48
3	0.08	1.55	1.47	−0.47
4	0.09	1.48	1.39	−0.44
5	0.09	0.96	0.87	−0.45
6	0.09	1.05	0.96	−0.42

Table 3. Analysis of variance for hydrazine electrooxidation on **hybrid 1**.

Source	Sum of Squares	df	Mean Square	F Value	p-value Prob > F	
Model	13.11	9	1.46	3.45	0.0333	significant
X_1	0.015	1	0.015	0.035	0.8546	
X_2	1.10	1	1.10	2.61	0.1374	
X_3	1.37	1	1.37	3.26	0.1013	
X_1X_2	5.41	1	5.41	12.83	0.0050	
X_1X_3	0.11	1	0.11	0.26	0.6208	
X_2X_3	0.61	1	0.61	1.44	0.2578	
X_1^2	0.75	1	0.75	1.77	0.2127	
X_2^2	0.17	1	0.17	0.40	0.5397	
X_3^2	0.29	1	0.29	0.70	0.4230	
Residual	4.22	10	0.42			
Lack of Fit	3.15	5	0.63	2.95	0.1299	not significant
Pure Error	1.07	5	0.21			
Cor Total	17.33	19				

Table 4. Optimum conditions by the CCD.

Solution Number	M_{KOH} (mg/L)	M_{Hyd} (mg/L)	V_c (μL)	Specific Activity (mA/cm^2)	Desirability
1	4.00	3.00	6.00	3.55324	0.833
2	4.00	2.99	6.00	3.53335	0.825
3	3.96	3.00	5.97	3.5024	0.814
4	3.91	3.00	6.00	3.46048	0.798
5	4.00	2.83	6.00	3.31695	0.744
6	3.66	3.00	6.00	3.22131	0.708
7	4.00	2.38	6.00	2.74377	0.530
8	0.20	0.22	0.50	2.20493	0.328
9	0.23	0.20	0.50	2.18912	0.322
10	0.20	0.20	6.00	2.18063	0.319

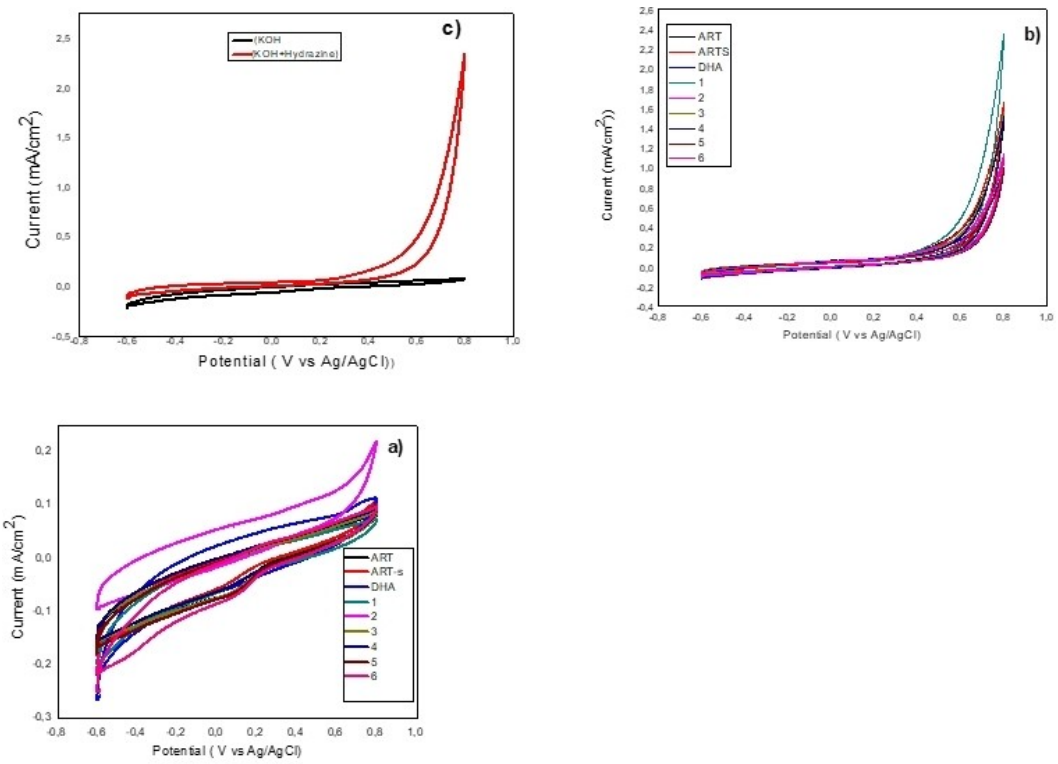

Figure 4. CV results of artemisinin-based catalysts in a) 1 M KOH and b) 1 M KOH + 0.5 M N_2H_4, c) (**1**) in comparison of 1 M KOH and 1 M KOH + 0.5 M Hydrazine at 50 mV s^{-1} scan rate of catalysts.

of artemisinin, dihydroartemisinin, artesunate, and artemether have been developed with the aim of increasing the pharmacological activity and the pharmacokinetic profile of the main drug (Figure 1).[45,46] Dihydroartemisinin is also found as anticancer agents against osteosarcoma, pancreatic, leukemic and lung cancer cells.[47]

Herein, we aimed to develop artemisinin based organic catalysts for hydrazine electrooxidation reaction as an anode catalyst.[31,48] By using optimized reaction conditions, a variety of artemisinin derivatives were synthesized. Then, electrooxidation performance was found via CV and the EIS. Moreover, optimum conditions for electrode preparation were found with Response Surface Methodology (**RSM**).

Results and Discussion

Synthesis

In order to synthesis of desired compounds, Steglich reaction was used. The reaction between artesunate and heterocyclic compounds including piperazine derivatives, piperidine derivatives and morpholine produced the artemisinin hybrid compounds with highest yields (Figure 2). Initially, (3R,5aS,6-R,8aS,9R,12R,12aR)-3,6,9-trimethyl decahydro-12 H-3,12-epoxy[1,2]dioxepino [4,3-i]isochroman-10-yl 4-morpholino-4-oxobutanoate **1** were synthesized in 54% yields by starting from the artesunate in the presence EDCI as a catalyst. When same reaction condition was used with piperidine, piperidine-artemisinin (**2**) was isolated in 46% yields. If artesunate was allowed to react with 1-(4-methoxybenzyl)piperazine in the presence EDCI/DMAP, desired corresponding compound (**3**) formed (47% yields). When ethyl piperazine-1-carboxylate was underwent to reaction, compound (**4**) was obtained in 93% yileds. 1-(4-chlorobenzyl)piperazine and 1-(4-fluorobenzyl)piperazine were reacted with artesunate for the formation of compounds **5** and **6**, 97% yields of **5** and 96% yields of **6** were isolated, respectively (Figure 2). The ^{1}H-NMR and ^{13}C-NMR spectrums of artemisinin hybrid molecules have characteristics peaks when compared with literature [46]. The characteristic peaks of artemisinin can be seen around 5.3 ppm as a doublet and around 5.7 ppm as a singlet. The ^{13}C-NMR spectra are very important for the identification of the carbonyl (C=O) peaks of our hybrid molecules. There are one ester's carbonyl peak and one amide's carbonyl peaks. These carbonyl peaks are shifted around 172 ppm and 169 ppm in the ^{13}C-NMR spectrum. The possible reaction mechanism was given in Figure 3.

Electrochemical evaluation

Hydrazine electrooxidation performances of **DHA**, **Artemisinin-ART**, **Artesunate- ARTS**, **Hybrid 1**, **Hybrid 2**, **Hybrid 3**, **Hybrid 4**, **Hybrid 5** and **Hybrid 6** catalysts were examined with CV analysis. CV measurements in 1 M KOH solution and 1 M KOH + 0.5 M N_2H_4 solution are given. The specific activity of DHA, ART, ARTS, 1 2, 3, 4, 5 and 6 artemisinin-based catalysts toward

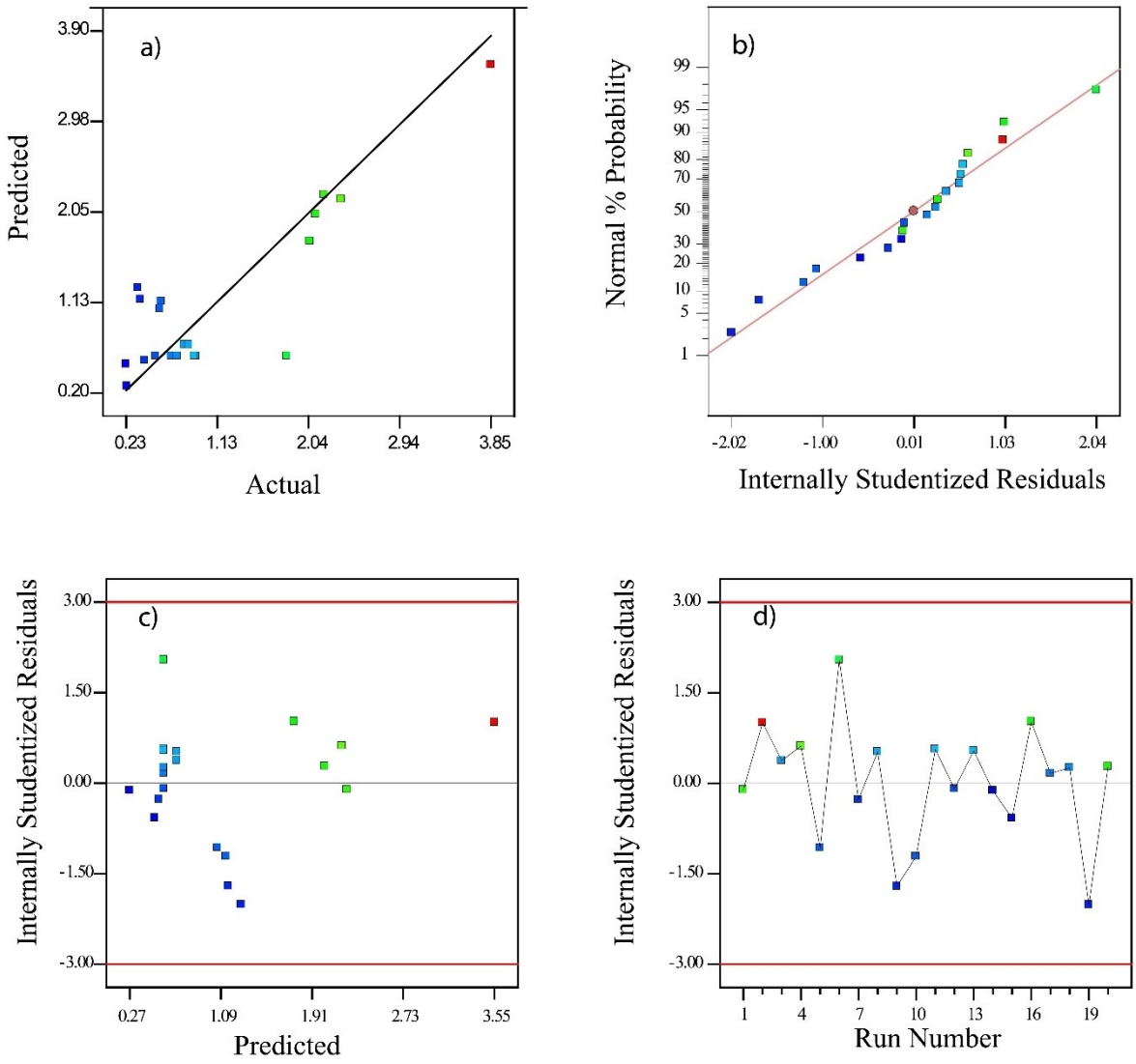

Figure 5. The actual-predicted and internally studentized residuals graphs were used to test the fit of the model

hydrazine electrooxidation obtained from CV results (Figure 4) were shown in Table 2. The parameters given in Table 2 are the current value at the total potential taken in 1 M KOH solution; indicates the total current value taken in a total of 0.5 M N_2H_4, while the normal current value indicates the difference between the current received in 1 M KOH and 0.5 M N_2H_4. The onset potential is found by using potential. The lower the onset potential means the faster the oxidation. When all molecules were compared, the highest performance artemisinin-based catalyst was shown as **hybrid 1** catalysts in hydrazine electrooxidation with 2.28 mA/cm^2, while the lowest performance was obtained from **ART** (Table 2). These results displayed that **hybrid 1** is a promising artemisinin-based catalyst for hydrazine electrooxidation.

CCD for hydrazine electrooxidation on (1) catalyst

A total of 20 sets of experiments were performed for obtaining optimum values of M_{KOH}, $M_{Hyd,}$ and V_c for hydrazine electrooxidation on **hybrid** (**1**). 5 of the 20 sets of experiments were conducted at the same points to determine the experimental errors, while the remaining 15 sets were performed at different points. The specific activity values for hydrazine electrooxidation on **hybrid** (**1**) at the points determined by the Design Expert 7.0 software were obtained by cyclic voltammetry. The quadratic equations proposed by the software for electrooxidation of hydrazine with **hybrid** (**1**) were given in Eq. 1 and Eq. 2 in terms of coded and real values.

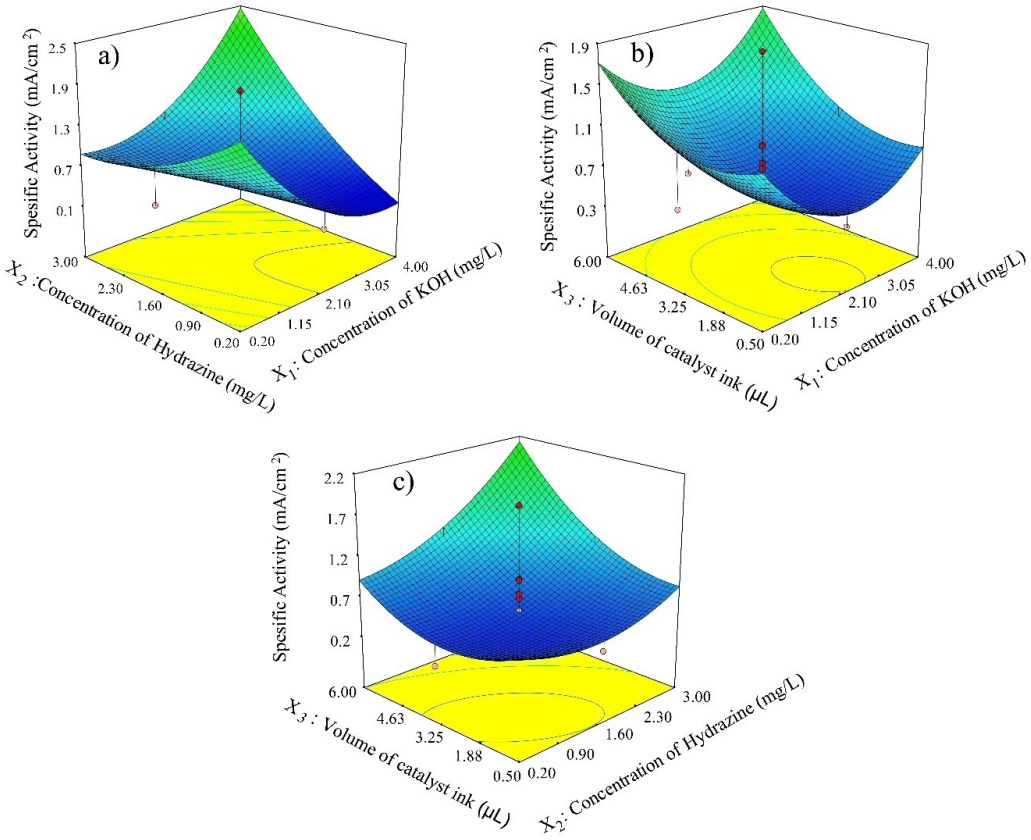

Figure 6. a) M_{KOH}, b) Mhyd, and c) Vc versus specific activity for hydrazine electrooxidation on **hybrid** (**1**)

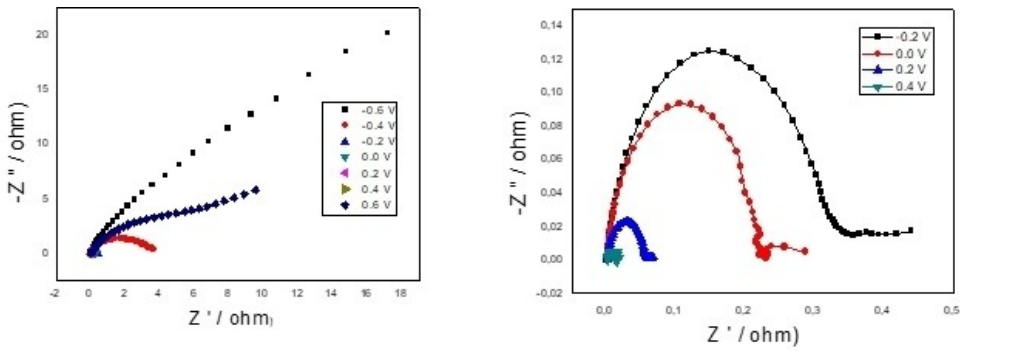

Figure 7. Nyquist plots derived from EIS measurements of **hybrid** 1 catalyst at different potentials

$$\text{Specific Activity for Hydrazine Electrooxidation} = +0.58 - 0.039^{*}X_1 + 0.33^{*}X_2 + 0.37^{*}X_3 + 0.82^{*}X_1{}^{*}X_2 + 0.12^{*}X_1{}^{*}X_3 + 0.28^{*}X_2{}^{*}X_3 + 0.52^{*}X_1^2 + 0.25^{*}X_2^2 + 0.33^{*}X_3^2 \quad (1)$$

$$\text{Spesific Activity for Hydrazine Electrooxidation} = +2.78565 - 1.19445^{*}M_{KOH} - 1.05108^{*}M_{Hyd} - 0.30810^{*}V_c + 0.30919^{*}M_{KOH}{}^{*}M_{Hyd} + 0.022435^{*}M_{KOH}{}^{*}V_c + 0.071578^{*}M_{Hyd}{}^{*}V_c + 0.14441^{*}M_{KOH}^2 + 0.12689^{*}M_{Hyd}^2 + 0.043267^{*}V_C^2 \quad (2)$$

The statistical significance of the model proposed by Design Expert 7.0 was revealed by analysis of variance (ANOVA)

and was given in Table 3. The regression coefficient of the proposed model was found to be 0.76, indicating that 24% of all variations could not be predicted by the proposed model. The p-value of the model proposed from the analysis of variance was determined as 0.0333, and since it is less than 0.05, the quadratic model is statistically significant at the 95% confidence interval [31]. Since the p values of model terms X_2 and X_3 are greater than 0.05, they are statistically insignificant but close to 0.1 indicates that these terms make a positive contribution to the predictive ability of the model. The p-value of the X_1X_2 term between binary interactions is less than 0.05 and is statistically significant. Although the other model terms are statistically insignificant, they were not excluded from the model because of their positive contribution to estimation. The p-value of the model's lack of fit test is 0.1299, showing that the model values and experimental data are in good agreement. In addition, the fact that the model has 3.45 F value supports this proposition. Model suitability was also verified with adequate precision. The adequate precision of the proposed quadratic model was determined as 7.151, and adequate precision values greater than 4 indicate that the proposed model could make accurate predictions within the design limits.[49]

The actual-predicted and internally studentized residuals graphs were used to test the fit of the model and are given in Figure 5. In Figure 5a, model values and actual values are compared. Most of the experimental points are scattered around the diagonal, except for some outliers (Runs 6, 9, and 19). The closeness of model values and actual values confirms the suitability of the proposed model for hydrazine electrooxidation on **hybrid 1**. The normal probability distributions of the residues for hydrazine electrooxidation were shown in Figure 5b. The residues showed a random distribution around the diagonal, indicating that the data set is normally distributed. Figure 5c demonstrates the internally studentized residual versus predicted values for hydrazine electrooxidation on **hybrid 1**. The studentized data were distributed between the theoretical $+3$ and -3 limits, indicating that the obtained data are not outliers. In addition, it was concluded from Figures 5b and **5c** that the data are suitable and that a mathematical transformation of specific activity values is not required. Figure 5d shows the distribution of the residues against the experimental numbers. As can be seen from Figure 5d, the residuals were randomly scattered and no recurring trend was detected in the distribution of the experiment points, indicating that the effects of V_c, $M_{KOH,}$ and M_{Hyd} on the specific activity are time-independent.

Response surface plots of independent variables namely M_{KOH}, $M_{hyd,}$ and V_c versus specific activity for hydrazine electrooxidation on **hybrid 1** was given in Figure 6. As can be seen in Figure 6a, when the M_{KOH} value increased from 0.2 mg/L to 2.1 mg/L, the specific activity decreased from 1.137 mA/cm^2 to 0.521 mA/cm^2, and with the increase of M_{KOH} up to 4 mg/L, the specific activity increased to 1.4339 mA/cm^2. KOH was used as supporting electrolyte and it was concluded from the design results that the supporting electrolyte could not provide enough ions up to 0.2 mg/L of M_{KOH}. In addition, at 2.1 mg/L M_{KOH} and 3.25 μL V_c, the specific activity for hydrazine electrooxidation increased from 0.494 to 1.158 mg/L with the increase of M_{Hyd} from 0.2 mg/L to 3 mg/L (Figure 6b). The increase in the specific activity was attributed to the increase in the number of hydrazine molecules adsorbed on the **hybrid 1** surface. As can be seen in Figure 6c, the specific activity sharply increased from 0.534 to 1.275 mA/cm^2 as the V_c value was increased from 0.5 μl to 6 μL in the solution consisting of 2.1 mg/L KOH and 1.6 mg/L hydrazine. This was attributed to an increase in the number of hydrazine molecules bound to the surface, with the increase in the amount of **hybrid 1** transferred to the GCE surface.

Optimum M_{KOH}, $M_{Hyd,}$ and V_c values for maximum specific activity toward hydrazine electrooxidation on **hybrid 1** were determined by using the numerical optimization method in Design Expert 7.0. M_{KOH}, $M_{Hyd,}$ and V_c parameters were optimized between their maximum and minimum values in Table S1 and the solutions suggested as a result of numerical optimization with Design Expert 7.0 software are summarized in Table 4. Among these solutions, the numerical solution proposal number 1 with the highest desirability value of 0.833 was determined as the optimum points for hydrazine electrooxidation on **hybrid 1**. While optimum values for M_{KOH}, $M_{hyd,}$ and V_c were determined as 4 mg/L, 3 Mg/L, and 6 μL, respectively, the specific activity for hydrazine electrooxidation was estimated as 3.55324 mA/cm^2 under these conditions.

According to the RSM optimization, experimental parameters were obtained as 4 M KOH + 3 M N_2H_4. At these optimum conditions EIS measurements were obtained. To determine the best resistance to hydrazine electrooxidation, EIS measurements were taken at different potentials in the range of -0.6 V-0.8 V, and Nyquist plots were used. These graphs are generally known as semicircles, where the load transfer resistance increases as the diameter of the circle decreases. The charge transfer resistance (Rct) is associated with the diameter of the semicircle because as the diameter decreases, Rct decreases, and so the catalytic activity increases.[50] As seen in Figure 7, the Nyquist plot taken at the potential of 0.4 V displayed the best electrochemical resistance. This result indicates that **hybrid 1** catalyst has the highest activity in hydrazine electrooxidation reaction.

Conclusions

In the present study, novel artemisinin hybrid molecules (1-6) were synthesized via Steglich esterification reaction, and characterized. The yields of the isolated products ranged from 46% to 96% yields. After the characterization, hydrazine electrooxidation measurements of new (**1**–**6**) artemisinin-based catalysts and artemisinin, dihydroartemisinin, artesunate were performed in 1 M KOH + 0.5 M N_2H_4 solution by using CV and EIS. In addition, optimum conditions for electrode preparation were investigated with Response Surface Methodology (**RSM**). The highest performance was obtained by **hybrid 1** catalysts as 2.28 mA/cm^2 to hydrazine electrooxidation. As a result, artemisinin-based hybrid molecules could be an alternative anode catalyst for a direct hydrazine fuel cell.

Supporting Information Summary

Supporting information (PDF) includes the detailed experimental section and NMR spectra.

Acknowledgements

The authors thank to Eskisehir Osmangazi University BAP (Project No: FOA-2021-2203) for chemicals and solvents. The author (A. Kivrak) would like to acknowledge networking contribution by the COST Action CA17104 "New diagnostic and therapeutic tools against multidrug resistant tumours".

Conflict of Interest

The authors have no competing interests to declare that are relevant to the content of this article.

Data Availability Statement

Data sharing is not applicable to this article as no new data were created or analyzed in this study.

Keywords: Anode catalyst · Artemisinin · Electrooxidation · Energy · Heterocycles · RSM · Organocatalysis

[1] O. Santiago, E. Navarro, M. A. Raso, T. J. Leo, *Appl. Energy* **2016**, *179*, 497–522.
[2] D. Ş. Armeanu, Ş. C. Gherghina, G. Pasmangiu, *Energies* **2019**, *12*(19), 3704.
[3] C. Liao, J. T. Erbaugh, A. C. Kelly, A. Agrawal, *Renewable Sustainable Energy Rev.* **2021**, *145*, 111063.
[4] W. Liu, Y. T. Gong, W. B. Wu, W. S. Yang, C. M. Liu, Y. L. Deng, Z. S. Chao, *ChemSusChem* **2018**, *11*, 2229–2238.
[5] M. Park, T. Lee, B. S. Kim, *Nanoscale* **2013**, *5*, 12255–12260.
[6] A. Kivrak, C. Zobi, Y. Torlak, Y. Camlisoy, M. Kus, H. Kivrak, *Appl. Organomet. Chem.* **2018**, *32*(10), e4512.
[7] J. Deng, X. Li, S. Imhanria, K. Chen, X. Deng, W. Wang, *Electrochim. Acta* **2021**, *384*, 138417.
[8] M. Z. F. Kamarudin, S. K. Kamarudin, M. S. Masdar, W. R. W. Daud, *Int. J. Hydrogen Energy* **2013**, *38*, 9438–9453.
[9] F. Q. Chu, X. F. Chu, S. Zhang, H. H. Zhu, Y. R. Ren, J. J. Han, R. G. Xie, B. C. Lin, J. N. Ding, *ChemistrySelect* **2019**, *4*, 5269–5275.
[10] R. K. Arun, V. Gupta, P. Singh, G. Biswas, N. Chanda, *ChemistrySelect* **2019**, *4*, 152–159.
[11] A. Caglar, B. Ulas, O. Sahin, H. Kivrak, *Int. J. Energy Res.* **2019**, *43*, 8204–8216.
[12] T. Asset, A. Roy, T. Sakamoto, M. Padilla, I. Matanovic, K. Artyushkova, A. Serov, F. Maillard, M. Chatenet, K. Asazawa, H. Tanaka, P. Atanassov, *Electrochim. Acta* **2016**, *215*, 420–426.
[13] G. Feng, Y. Kuang, P. S. Li, N. Han, M. Sun, G. X. Zhang, X. M. Sun, *Adv. Sci.* **2017**, *4*, 1600179.
[14] M. S. Rahaman, S. Tulaphol, M. A. Hossain, J. B. Jasinski, N. Sun, A. George, B. A. Simmons, T. Maihom, M. Crocker, N. Sathitsuksanoh, *Fuel* **2022**, *310*, 122459.
[15] C. Rice, R. I. Ha, R. I. Masel, P. Waszczuk, A. Wieckowski, T. Barnard, *J. Power Sources* **2002**, *111*, 83–89.
[16] C. A. Lopez-Rico, J. Galindo-de-la-Rosa, L. Alvarez-Contreras, J. Ledesma-Garcia, M. Guerra-Balcazar, L. G. Arriaga, N. Arjona, *ChemistrySelect* **2016**, *1*, 3054–3062.
[17] A. Demirbas, *D. Energy Sources Part A* **2008**, *30*, 529–535.
[18] Y. Paik, S. S. Kim, O. H. Han, *Angew. Chem. Int. Ed.* **2008**, *47*, 94–96.
[19] M. C. L. Santos, L. C. Nunes, L. M. G. Silva, A. S. Ramos, F. C. Fonseca, R. F. B. de Souza, A. O. Neto, *ChemistrySelect* **2019**, *4*, 11430–11434.
[20] A. Benvidi, P. Kakoolaki, H. R. Zare, R. Vafazadeh, *Electrochim. Acta* **2011**, *56*, 2045–2050.
[21] Y. C. Wang, Q. Wang, L. Y. Wan, Y. Han, Y. H. Hong, L. Huang, X. D. Yang, Y. S. Wang, K. Zaghib, Z. Y. Zhou, *J. Colloid Interface Sci.* **2020**, *563*, 27–32.
[22] B. Filanovsky, E. Granot, I. Presman, I. Kuras, F. Patolsky, *J. Power Sources* **2014**, *246*, 423–429.
[23] R. Crisafulli, V. V. S. de Barros, F. E. R. de Oliveira, T. D. Rocha, S. Zignani, L. Spadaro, A. Palella, J. A. Dias, J. J. Linares, *App. Cat. B-Environmental* **2018**, *236*, 36–44.
[24] W. Jin, J. G. Liu, Y. T. Wang, Y. F. Yao, J. Gu, Z. G. Zou, *Int. J. Hydrogen Energy* **2013**, *38*, 10992–10997.
[25] X. L. Yan, F. H. Meng, Y. Xie, J. G. Liu, Y. Ding, *Sci. Rep.* **2012**, *2*(1), 1–7.
[26] B. Ulas, A. Caglar, A. Kivrak, H. Kivrak, *Chem. Pap.* **2019**, *73*, 425–434.
[27] L. X. Chen, L. Y. Jiang, A. J. Wang, Q. Y. Chen, J. J. Feng, *Electrochim. Acta* **2016**, *190*, 872–878.
[28] A. Zadick, J. F. Petit, V. Martin, L. Dubau, U. B. Demirci, C. Geantet, M. Chatenet, *ACS Catal.* **2018**, *8*, 3150–3163.
[29] M. Abdolmaleki, I. Ahadzadeh, H. Goudarziafshar, *Int. J. Hydrogen Energy* **2017**, *42*, 15623–15631.
[30] K. Ojha, E. M. Farber, T. V. Burshtein, D. Eisenberg, *Angew. Chem. Int. Ed.* **2018**, *57*, 17168–17172; *Angew. Chem.* **2018**, *130*, 17414–17418.
[31] O. F. Er, B. Ulas, O. Ozok, A. Kivrak, H. Kivrak, *J. Electroanal. Chem.* **2021**, 888, 115218.
[32] H. Rostami, A. Omrani, A. A. Rostami, A. Emamgholizadeh, *Ionics* **2015**, *21*, 1073–1080.
[33] K. Akbar, J. H. Kim, Z. Lee, M. Kim, Y. Yi, S. H. Chun, *NPG Asia Mater.* **2017**, *9*(5), e378-e378.
[34] J. Ding, P. Kannan, P. Wang, S. Ji, H. Wang, Q. Liu, H. Gai, F. Liu, R. Wang, *J. Power Sources* **2019**, *413*, 209–215.
[35] M. B. Askari, P. Salarizadeh, H. Beitollahi, S. Tajik, A. Eshghi, S. Azizi, *Mater. Chem. Phys.* **2022**, *275*, 125313.
[36] Y. Y. Ma, H. Wang, J. Key, S. Ji, W. Z. Lv, R. F. Wang, *J. Power Sources* **2015**, *300*, 344–350.
[37] A. Gluszynska, *Euro. J. Med. Chem.* **2015**, *94*, 405–426.
[38] M. A. S. Algso, A. Kivrak, *Chem. Pap.* **2019**, *73*, 977–985.
[39] T. P. Singh, O. M. Singh, *Mini-Rev. Med. Chem.* **2018**, *18*, 9–25.
[40] B. B. Carbas, A. Kivrak, M. Zora, A. M. Onal, *J. Electroanal. Chem.* **2012**, *677*, 9–14.
[41] R. El Mouhi, S. El Khattabi, M. Hachi, A. Fitri, A. T. Benjelloun, M. Benzakour, M. McHarfi, M. Bouachrine, *Res. Chem. Intermed.* **2019**, *45*, 1327–1340.
[42] P. R. Nitha, V. Jayadev, S. C. Pradhan, V. V. Divya, C. H. Suresh, J. John, S. Soman, A. Ajayaghosh, *Asian J. Chem.* **2020**, *15*, 3503–3512.
[43] E. Kavak, D. Mutlu, O. Ozok, S. Arslan, A. Kivrak, *Nat. Prod. Res.* **2020**, 1–9.
[44] A. Malaviya, K. Malhotra, A. Agarwal, K. Saikia, *Human Health* **2019**, *1*, 347.
[45] N. Ma, Z. Y. Zhang, F. L. Liao, T. L. Jiang, Y. Y. Tu, *Pharm. Therap* **2020**, *216*, 107658.
[46] O. Ozok, E. Kavak, A. Kivrak, *Nat. Prod. Res.* **2021**, 1–7.
[47] D. J. Newman, G. M. Cragg, K. M. Snader, *Nat. Prod. Rep.* **2000**, *17*, 215–234.
[48] O. Ozok, E. Kavak, O. F. Er, H. Kivrak, A. Kivrak, *Int. J. Hydrogen Energy* **2020**, *45*, 28706–28715.
[49] A. Aggarwal, H. Singh, P. Kumar, M. Singh, *J. Mater. Process. Technol.* **2008**, *200*, 373–384.
[50] S. Durairaj, S. Vaithilingam, *J. Electroanal. Chemistry* **2017**, *787*, 55–65.

Submitted: April 5, 2022
Accepted: May 6, 2022